Title

Atmospheric Chemistry of Methyl and Ethyl N,N,N′,N′-Tetramethylphosphorodiamidate and O,S-Dimethyl Methylphosphonothioate

Journal

The Journal of Physical Chemistry A, 117(43)

ISSN

1089-5639

Authors

Aschmann, Sara M
Atkinson, Roger

Publication Date

2013-10-31

DOI

10.1021/jp407702w

Peer reviewed

THE JOURNAL OF PHYSICAL CHEMISTRY A

Article

pubs.acs.org/JPCA

Atmospheric Chemistry of Methyl and Ethyl *N,N,N′,N′*-Tetramethylphosphorodiamidate and *O,S*-Dimethyl Methylphosphonothioate

Sara M. Aschmann and Roger Atkinson*

Air Pollution Research Center, University of California, Riverside, California 92521, United States

Supporting Information

ABSTRACT: Rate constants for the reactions of OH radicals with methyl *N,N,N′,N′*-tetramethylphosphorodiamidate [$CH_3OP(O)[N(CH_3)_2]_2$; MTMPDA], ethyl *N,N,N′,N′*-tetramethylphosphorodiamidate [$C_2H_5OP(O)[N(CH_3)_2]_2$; ETMPDA], and *O,S*-dimethyl methylphosphonothioate [$CH_3OP(O)(CH_3)SCH_3$; OSDMMP] have been measured over the temperature range 281−349 K at atmospheric pressure of air using a relative rate method. The rate expressions obtained were 4.96×10^{-12} $e^{(1058\pm71)/T}$ cm^3 $molecule^{-1}$ s^{-1} (1.73×10^{-10} cm^3 $molecule^{-1}$ s^{-1} at 298 K) for OH + MTMPDA, 4.46×10^{-12} $e^{(1144\pm95)/T}$ cm^3 $molecule^{-1}$ s^{-1} (2.07×10^{-10} cm^3 $molecule^{-1}$ s^{-1} at 298 K) for OH + ETMPDA, and 1.31×10^{-13} $e^{(1370\pm229)/T}$ cm^3 $molecule^{-1}$ s^{-1} (1.30×10^{-11} cm^3 $molecule^{-1}$ s^{-1} at 298 K) for OH + OSDMMP. The rate constant for OH + OSDMMP was independent of O_2 content over the range 2.1−71% O_2 at 296 ± 2 K. In addition, rate constants for the reactions of NO_3 radicals and O_3 with MTMPDA, of $(1.4 \pm 0.1) \times 10^{-12}$ cm^3 $molecule^{-1}$ s^{-1} and $<3.5 \times 10^{-19}$ cm^3 $molecule^{-1}$ s^{-1}, respectively, were measured at 297 ± 2 K. Products of the OH radical- and, for MTMPDA, NO_3 radical-initiated reactions were investigated using gas chromatography and in situ atmospheric pressure ionization mass spectrometry. A product of molecular weight 180 was observed from the OH and NO_3 radical-initiated reactions of MTMPDA, and this is attributed to $CH_3OP(O)[N(CH_3)_2]N(CH_3)CHO$. Similarly, a product of molecular weight 194 was observed from the OH + ETMPDA reaction and attributed to $C_2H_5OP(O)[N(CH_3)_2]N(CH_3)CHO$. Possible reaction mechanisms are discussed.

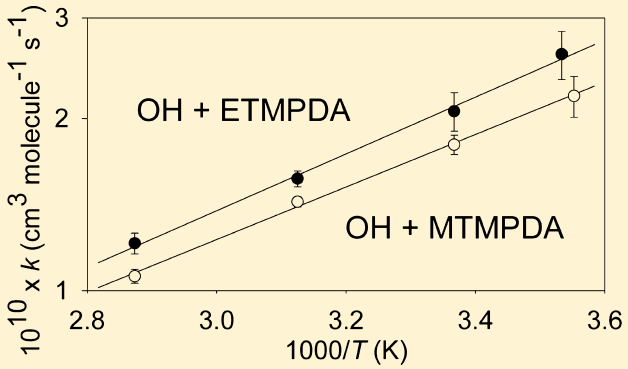

INTRODUCTION

Organophosphorus compounds are widely used as pesticides[1] and may be released into the troposphere where they can undergo transport and photolysis (at wavelengths >290 nm) and reactions with OH radicals, NO_3 radicals, and O_3.[2] The kinetics of the gas-phase reactions of a number of organophosphorus compounds of structure $(RO)_nP(X)(SR)_{3-n}$ and $(RO)_2P(X)Y$, where $R = CH_3$, C_2H_5, or $CH(CH_3)_2$, X = O or S, and Y = H, CH_3, C_2H_5, NH_2, $NHCH_3$, $N(CH_3)_2$, $OCH{=}CCl_2$, OC_5NHCl_3, or Cl, with OH radicals, NO_3 radicals, and O_3 have been studied.[3−17] Under atmospheric conditions, reaction with OH radicals was calculated to dominate for the alkyl phosphates, phosphorothioates, phosphonates, and phosphonothioates.[4−6,8,10,13,15,16] For dimethyl phosphonate [$(CH_3O)_2P(O)H$; DMHP], dimethyl methylphosphonate [$(CH_3O)_2P(O)CH_3$; DMMP], dimethyl ethylphosphonate [$(CH_3O)_2P(O)C_2H_5$; DMEP], diethyl methylphosphonate [$(C_2H_5O)_2P(O)CH_3$; DEMP], diethyl ethylphosphonate [$(C_2H_5O)_2P(O)C_2H_5$; DEEP], triethyl phosphate [$(C_2H_5O)_3PO$; TEP], isopropyl methyl methylphosphonate [$(CH_3)_2CHOP(O)(CH_3)OCH_3$; IMMP], *O,O*-diethyl methylphosphonothioate [$(C_2H_5O)_2P(S)CH_3$; DEMPT], *O,O,O*-triethyl phosphorothioate [$(C_2H_5O)_3PS$; TEPT], dimethyl *N,N*-dimethylphosphoroamidate [$(CH_3O)_2P(O)N(CH_3)_2$; DMDMPA], and dichlorvos [2,2-dichlorovinyl dimethyl phosphate, $(CH_3O)_2P(O)OCH{=}CCl_2$], rate constants for the OH radical reactions have been measured as a function of temperature[12−16] and product formation investigated.[8,10,13,15,16,18] These OH radical reactions all exhibit negative temperature dependencies, with values of B in $k = A\,e^{-B/T}$ ranging from −(474 ± 159) K for DMHP to −(1516 ± 149) K for the alkyl phosphates and phosphonates studied.[13−16] These OH radical reactions proceed by the initial formation of a complex (or complexes), which can back-decompose to reactants in competition with decomposition to products, with the barrier to back-decomposition to reactants being higher than that for decomposition to products.[12−16] Theoretical calculations[19,20] and product data[8,10,15] show that the reactions of alkyl phosphates and alkyl phosphonates [$(RO)_3PO$ and $(RO)_{3-x}P(O)R_x$, where R = alkyl] with OH radicals proceed mainly by H-atom abstraction from the −OR groups.

Received: August 1, 2013
Revised: September 25, 2013
Published: October 17, 2013

dx.doi.org/10.1021/jp407702w | *J. Phys. Chem. A* 2013, 117, 11038−11048

In this last of a series of studies of the atmospherically relevant reactions of model organophosphorus compounds, we have measured rate constants for the reactions of OH radicals with methyl *N*,*N*,*N*′,*N*′-tetramethylphosphorodiamidate [$CH_3OP(O)[N(CH_3)_2]_2$; MTMPDA], ethyl *N*,*N*,*N*′,*N*′-tetramethylphosphorodiamidate [$C_2H_5OP(O)[N(CH_3)_2]_2$; ETMPDA], and *O*,*S*-dimethyl methylphosphonothioate [$CH_3OP(O)(CH_3)SCH_3$; OSDMMP] over the temperature range 281−349 K at atmospheric pressure of air using a relative rate method. In addition, rate constants were measured at room temperature for the reaction of MTMPDA with NO_3 radicals and O_3, and products of the reactions of OH radicals with MTMPDA, ETMPDA, and OSDMMP were briefly investigated.

EXPERIMENTAL METHODS

Experiments were carried out at atmospheric pressure (∼735 Torr) in 7220 ± 400 L and ∼7500 L Teflon film chambers at room temperature, and in a ∼4500 L Teflon film bag inserted inside a 5870 L Teflon-coated cylindrical chamber fitted with a heating/cooling system allowing its temperature to be maintained to within ±1 K over the range ∼280−350 K.[15] These chambers were fitted with Teflon-coated fans to ensure rapid mixing of reactants during their introduction into the chamber and with black lamps for irradiation at >300 nm. The 7220 L Teflon chamber was interfaced to a PE SCIEX API III MS/MS direct air sampling, atmospheric pressure ionization tandem mass spectrometer (API-MS). All irradiations were carried out at a light intensity corresponding to an NO_2 photolysis rate of ∼0.14 min^{-1}.

Kinetic Studies. Rate constants for the reactions of OH radicals with MTMPDA, ETMPDA, and OSDMMP, and for NO_3 radicals with MTMPDA, were measured using relative rate techniques in which the concentrations of the organophosphorus compound and a reference compound (whose OH radical or NO_3 radical reaction rate constant is reliably known) were measured in the presence of OH or NO_3 radicals. The organophosphorus compounds can also undergo dark decay, and for the loss processes

$$\text{OH (or } NO_3\text{)} + \text{organophosphorus compound} \rightarrow \text{products} \quad (1)$$

$$\text{OH (or } NO_3\text{)} + \text{reference compound} \rightarrow \text{products} \quad (2)$$

$$\text{organophosphorus compound} \rightarrow \text{loss} \quad (3)$$

then,

$$\ln\left(\frac{[\text{organophosphorus}]_{to}}{[\text{organophosphorus}]_t}\right) - k_3(t - t_o) - D_t = \frac{k_1}{k_2}\left[\ln\left(\frac{[\text{reference}]_{t_o}}{[\text{reference}]_t}\right) - D_t\right] \quad (I)$$

where $[\text{organophosphorus}]_{to}$ and $[\text{reference}]_{to}$ are the concentrations of the organophosphorus compound and reference compound, respectively, at time t_o, $[\text{organophosphorus}]_t$ and $[\text{reference}]_t$ are the corresponding concentrations at time t, D_t is a factor to account for dilution caused by any additions to the chamber during the experiments (D_t = 0 for the OH radical reactions, and D_t = 0.0026 per N_2O_5 addition to the chamber in the NO_3 radical reactions), and k_1, k_2, and k_3 are the rate constants for reactions 1, 2, and 3, respectively.

Hydroxyl radicals were generated in the presence of NO by the photolysis of methyl nitrite in air at wavelengths >300 nm. The initial reactant concentrations (molecules cm^{-3}) employed for the OH radical reactions were CH_3ONO and NO, ∼2.4 × 10^{14} each, except in an experiment with 71 ± 3% O_2 content where the initial CH_3ONO and NO were ∼1.2 × 10^{14} each; reference compound, ∼(1.5−2.4) × 10^{13}; and MTMPDA and ETMPDA, ∼1.5 × 10^{13} or OSDMMP, ∼2.4 × 10^{13}. Irradiations were carried out for up to 13 min (MTMPDA), 12 min (ETMPDA), or 60 min (OSDMMP). Experiments were also conducted to measure the dark decay rates of MTMPDA and ETMPDA at each temperature studied, and for OSDMMP at 283 K. Photolysis of MTMPDA was also investigated, with 2.4 × 10^{15} molecules cm^{-3} of cyclohexane being present to scavenge ≥85% of any OH radicals formed.

Nitrate radicals were produced from the thermal decomposition of N_2O_5, and NO_2 was also included in the reactant mixtures. The initial reactant concentrations (molecules cm^{-3}) were MTMPDA, ∼1.5 × 10^{13}; 1-butene or *trans*-2-butene (the reference compounds), ∼2.4 × 10^{13}; NO_2, (4.8−9.6) × 10^{13}; and three additions of N_2O_5 (each addition corresponding to (5.2−8.0) × 10^{12} molecules cm^{-3} of N_2O_5 in the chamber) were made to the chamber during an experiment.

The concentrations of the organophosphorus compounds and reference compounds were measured during the experiments by gas chromatography with flame ionization detection (GC-FID). For the analyses of α-pinene, 1,3,5-trimethylbenzene, *n*-decane, di-*n*-butyl ether, MTMPDA, ETMPDA, and OSDMMP, 100 cm^3 volume gas samples were collected from the chamber onto Tenax-TA solid adsorbent, with subsequent thermal desorption at ∼205 °C onto a 30 m DB-1701 megabore column held at −40 or 0 °C and then temperature programmed at 8 °C min^{-1}. For the analyses of 1-butene and *trans*-2-butene, gas samples were collected from the chamber into a 100 cm^3 volume all-glass gastight syringe and transferred via a 1 cm^3 gas sampling loop onto a 30 m DB-5 megabore column initially held at −25 °C and then temperature programmed at 8 °C min^{-1}. On the basis of replicate analyses in the chamber in the dark, the analytical uncertainties for the organophosphorus compounds and the reference compounds were typically ≤3% and ≤2%, respectively.

The rate constant, or upper limit thereof, for the reaction of MTMPDA with O_3 was determined by monitoring the decay of MTMPDA in the presence of a known concentration of O_3,[8,10,15] with cyclohexane being present to scavenge ≥85% of any OH radicals formed. The initial reactant concentrations (molecules cm^{-3}) were MTMPDA, ∼1.5 × 10^{13}; O_3, 3.19 × 10^{13}; and cyclohexane, 2.4 × 10^{15}. O_3 concentrations were measured during the 5.1 h duration reaction by ultraviolet absorption, and the concentrations of MTMPDA were measured by GC-FID as described above.

Product studies. *Analyses by GC.* In addition to GC-FID analyses conducted during the kinetic experiments, samples were collected from the OH radical-initiated reactions of MTMPDA and ETMPDA onto Tenax-TA solid adsorbent (MTMPDA) or solid phase microextraction (SPME) fibers (ETMPDA) and analyzed using combined gas chromatography−mass spectrometry (GC-MS). A 60 m DB-5 column in an Agilent 6890N GC interfaced to an Agilent 5975 Inert XL Mass Selective Detector (MTMPDA) or a 30 m HP-5MS column in an Agilent 6890N GC interfaced to an Agilent 5973N Mass Selective Detector (ETMPDA) was used,

dx.doi.org/10.1021/jp407702w | J. Phys. Chem. A 2013, 117, 11038−11048

Table 1. Rate Constant Ratios k_1/k_2 and Rate Constants k_1 for the Reactions of OH Radicals with MTMPDA, ETMPDA, and OSDMMP

organophosphorus compound	temperature (K)	$10^6 \times k_3$ (s^{-1})	reference compound	k_1/k_2[a]	$10^{11} \times k_1$ (cm^3 $molecule^{-1}$ s^{-1})[b]
MTMPDA	281.5 ± 1	5.2	α-pinene	3.84 ± 0.31	21.9 ± 1.8
	297 ± 1	4.2	α-pinene	3.42 ± 0.13	18.0 ± 0.7
	297 ± 1	4.2	1,3,5-TMB	2.93 ± 0.07	16.6 ± 0.4
	320 ± 1	2.5	α-pinene	3.03 ± 0.06	14.3 ± 0.3
	348 ± 1	4.2	α-pinene	2.50 ± 0.07	10.6 ± 0.3
ETMPDA	283 ± 1	9.9	α-pinene	4.58 ± 0.43	25.9 ± 2.5
	297 ± 1	3.6	α-pinene	3.92 ± 0.30	20.6 ± 1.6
	320 ± 1	7.2	α-pinene	3.32 ± 0.10	15.7 ± 0.5
	348 ± 1	7.9	α-pinene	2.85 ± 0.10	12.1 ± 0.5
OSDMMP	296 ± 2		*n*-decane	1.26 ± 0.07[c]	1.37 ± 0.08
	320 ± 1		di-*n*-butyl ether	0.376 ± 0.019	0.920 ± 0.047
	349 ± 1		di-*n*-butyl ether	0.315 ± 0.020	0.678 ± 0.044

[a]Indicated errors are two least-squares standard deviations. At 297 ± 1 K, k_1(OH + MTMPDA)/k_2(OH + pinene) = 3.30 ± 0.15 using the combined data with α-pinene and 1,3,5-trimethylbenzene as reference compounds (see Figure 2), leading to k_1(OH + MTMPDA) = (1.73 ± 0.08) × 10^{-10} cm^3 $molecule^{-1}$ s^{-1}. [b]Placed on an absolute basis using rate constants k_2 of k_2(OH + α-pinene) = 1.21 × 10^{-11} $e^{436/T}$ cm^3 $molecule^{-1}$ s^{-1},[2] k_2(OH + 1,3,5-trimethylbenzene) = 5.67 × 10^{-11} cm^3 $molecule^{-1}$ s^{-1} at 297 K,[2] k_2(OH + *n*-decane) = 1.09 × 10^{-11} cm^3 $molecule^{-1}$ s^{-1} at 296 K,[2] and k_2(OH + di-*n*-butyl ether) = 6.29 × 10^{-18} T^2 $e^{1164/T}$ cm^3 $molecule^{-1}$ s^{-1}.[21] [c]Independent of O_2 content over the range 2.1−71% O_2 (see Figure 4).

operated in positive chemical ionization mode with methane as the reagent gas.

Experiments with API-MS analyses. In these experiments (NO_3 + MTMPDA, OH + MTMPDA, OH + ETMPDA, and OH + OSDMMP), the chamber contents were sampled through a 25 mm diameter × 75 cm length Pyrex tube at ∼20 L min^{-1} directly into the API mass spectrometer source. The operation of the API-MS in the MS (scanning) and MS/MS (with collision activated dissociation) modes has been described previously,[8,10,15] and both positive and negative ion modes were used in this work. In positive ion mode, protonated water hydrates ($H_3O^+(H_2O)_n$) generated by the corona discharge in the chamber diluent air were responsible for the protonation of analytes, and the ions that were mass analyzed were mainly protonated molecular ions ($[M + H]^+$) and their protonated homo- and heterodimers.[8,10,15] In negative ion mode, negative ions are generated by the negative corona around the discharge needle, and under the conditions employed, O_2^-, NO_2^-, and NO_3^- were the major relevant negative ions. Instrument tuning and operation were designed to induce cluster formation.

For the OH radical reactions, the initial concentrations of CH_3ONO, NO, and organophosphorus compound were ∼(2.4−4.8) × 10^{13}, ∼(2.4−4.8) × 10^{13}, and (0.8−2.4) × 10^{13} molecules cm^{-3}, respectively, and irradiations were carried out for up to 1 min (MTMPDA), 5 min (ETMPDA), or 16 min (OSDMMP). For the NO_3 + MTMPDA reaction, the initial concentrations of MTMPDA and NO_2 were ∼8 × 10^{12} and ∼2.4 × 10^{13} molecules cm^{-3}, respectively, and one addition of N_2O_5, corresponding to 3.1 × 10^{12} molecules cm^{-3} of N_2O_5 in the chamber, was made during the experiment.

Chemicals. The chemicals used, and their stated purities, were di-*n*-butyl ether (99+%), *n*-decane (99+%), (+)-α-pinene (99+%), and 1,3,5-trimethylbenzene (98%), Aldrich; methyl *N*,*N*,*N*′,*N*′-tetramethylphosphorodiamidate [$CH_3OP(O)[N(CH_3)_2]_2$; MTMPDA] and *O*,*S*-dimethyl methylphosphonothioate [$CH_3OP(O)(CH_3)SCH_3$; OSDMMP] (90% purity, with 10% of a lower volatility compound of molecular weight 156, presumably $(CH_3S)_2P(O)CH_3$, which was completely separated from OSDMMP in the GC-FID and GC-MS analyses and therefore of no consequence for the kinetic experiments), Hestia Laboratories, Inc.; ethyl *N*,*N*,*N*′,*N*′-tetramethylphosphorodiamidate [$C_2H_5OP(O)[N(CH_3)_2]_2$; ETMPDA], MRI-Global; and 1-butene (99%), *trans*-2-butene (≥95%), and NO (≥99.0%), Matheson Gas Products. Methyl nitrite and N_2O_5 were prepared and stored as described previously,[8,10,15] and O_3 in O_2 diluent was generated using a Welsbach T-408 ozone generator. NO_2 was prepared as needed by reacting NO with an excess of O_2.

RESULTS

Photolysis and Dark Reactions. The measured gas-phase concentrations of MTMPDA and ETMPDA were observed to decrease monotonically in the dark over periods of 5.0−6.0 h, with the decay rate depending on chamber and temperature. The dark decay rates of MTMPDA and ETMPDA in the ∼4500 L Teflon bag are listed in Table 1 for the temperatures employed. The dark decay rate of MTMPDA in the ∼7500 L Teflon chamber used for the NO_3 radical and O_3 kinetic experiments and for investigation of photolysis of MTMPDA was (7.0 ± 1.9) × 10^{-6} s^{-1} over a period of 6.0 h, where (as elsewhere unless noted otherwise) the errors are two least-squares standard deviations. The MTMPDA decay rate in a 4.1 h duration experiment in which MTMPDA was irradiated for four 15 min intervals was (10.5 ± 1.9) × 10^{-6} s^{-1}, within the combined experimental uncertainties of the measured dark decay in this chamber. Since the total irradiation periods during the OH radical reaction rate constant determinations were ≤12 min, photolysis of MTMPDA was of no importance during our kinetic experiments, and the same was assumed to be the case for ETMPDA.

Replicate analyses in the dark prior to reaction showed no evidence for any dark decays of OSDMMP at any of the temperatures studied. However, while replicate analyses postreaction also showed no evidence for dark decays of OSDMMP at ≥296 K, significant postreaction dark decays of OSDMMP were observed at 283−284 K, of (1.0−2.3) × 10^{-5} s^{-1}.

Rate Constant for Reaction of O_3 with MTMPDA. In the presence of an average O_3 concentration of 3.02 × 10^{13}

dx.doi.org/10.1021/jp407702w | J. Phys. Chem. A 2013, 117, 11038−11048

molecules cm^{-3} and with 2.4×10^{15} molecules cm^{-3} of cyclohexane present to scavenge ≥85% of any OH radicals formed, a MTMPDA decay rate of $(8.6 \pm 1.7) \times 10^{-6}$ s^{-1} was observed over a reaction period of 5.1 h. This MTMPDA decay rate in the presence of O_3 was very similar to the dark decay rate in this chamber in the absence of O_3 of $(7.0 \pm 1.9) \times 10^{-6}$ s^{-1}, thereby showing no evidence for reaction with O_3. Attributing all of the observed decay rate in the presence of O_3 to reaction with O_3 results in an upper limit to the rate constant of

$$k(O_3 + \text{MTMPDA}) < 3.5 \times 10^{-19} \text{ cm}^3 \text{ molecule}^{-1} \text{ s}^{-1} \text{ at } 297 \pm 2 \text{ K}$$

Rate Constant for the Reaction of NO_3 Radicals with MTMPDA. In a N_2O_5−NO_3−NO_2−MTMPDA−1-butene−air mixture, MTMPDA was observed to be significantly more reactive than 1-butene, and hence *trans*-2-butene was used in subsequent experiments. The experimental data from reacting N_2O_5−NO_3−NO_2−MTMPDA−*trans*-2-butene−air mixtures are plotted in accordance with eq I in Figure 1. A least-squares

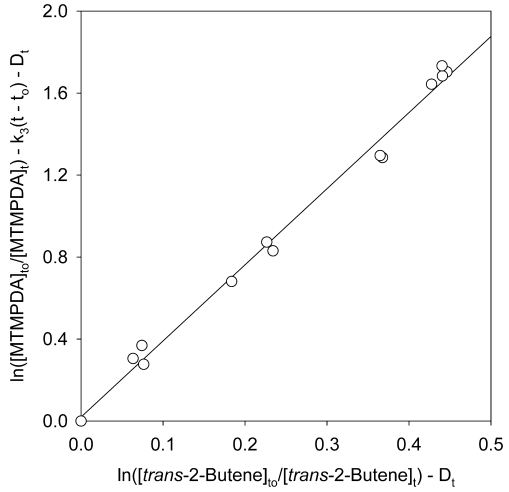

Figure 1. Plot of eq I for the reaction of NO_3 radicals with methyl *N,N,N′,N′*-tetramethylphosphorodiamidate (MTMPDA) at 296 ± 2 K, with *trans*-2-butene as the reference compound. Experiments were carried out in a ∼7500 L Teflon chamber.

analysis of these data leads to the rate constant ratio k_1/k_2 = 3.71 ± 0.21. This rate constant ratio is placed on an absolute basis by use of a rate constant at 297 K for reaction of NO_3 radicals with *trans*-2-butene of $k_2 = 3.89 \times 10^{-13}$ cm^3 $molecule^{-1}$ s^{-1},[2] resulting in

$$k_1(NO_3 + \text{MTMPDA}) = (1.4 \pm 0.1) \times 10^{-12} \text{ cm}^3 \text{ molecule}^{-1} \text{ s}^{-1} \text{ at } 297 \pm 2 \text{ K}$$

where the indicated error is two least-squares standard deviations and does not include the uncertainty in the rate constant k_2.

Rate Constants for the Reactions of OH Radicals with MTMPDA, ETMPDA, and OSDMMP. The data obtained from irradiations of CH_3ONO−NO−organophosphorus compound−reference compound−air mixtures are plotted in accordance with eq I in Figures 2 (MTMPDA), 3 (ETMPDA), and 4 and 5 (OSDMMP). The rate constants for OH + MTMPDA at 281.5 ± 1 K and for OH + ETMPDA at 283 ± 1

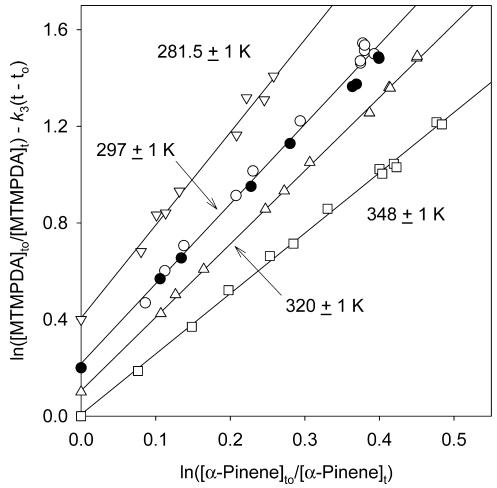

Figure 2. Plots of eq I for the reactions of OH radicals with methyl *N,N,N′,N′*-tetramethylphosphorodiamidate (MTMPDA) at 281.5 ± 1, 297 ± 1, 320 ± 1, and 348 ± 1 K, with α-pinene as the reference compound. Experiments were carried out in a ∼4500 L Teflon chamber. The MTMPDA data at 320 ± 1, 297 ± 1, and 281.5 ± 1 K have been displaced vertically by 0.10, 0.20, and 0.40 units, respectively, for clarity. The open symbols are with α-pinene as the reference compound; those at 297 ± 1 K shown as ● are with 1,3,5-trimethylbenzene as the reference compound, and the measured values of $\ln([\text{1,3,5-trimethylbenzene}]_{to}/[\text{1,3,5-trimethylbenzene}]_t)$ have been converted to $\ln([\alpha\text{-pinene}]_{to}/[\alpha\text{-pinene}]_t)$ by multiplication by 0.926 (the ratio of the rate constants for reaction with OH radicals). The solid line through the 297 ± 1 K data is a least-squares fit to the entire data set at that temperature, with $k_1(\text{OH} + \text{MTMPDA})/k_2(\text{OH} + \alpha\text{-pinene}) = 3.30 \pm 0.15$.

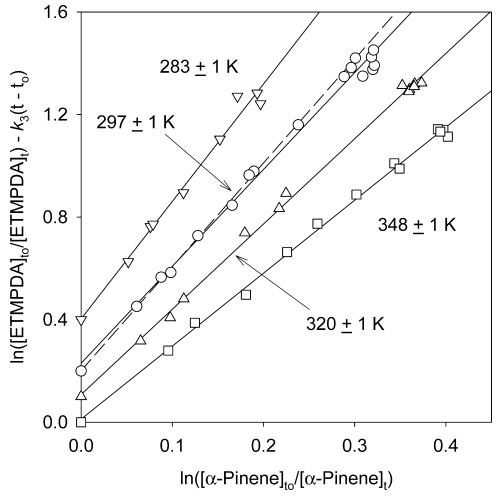

Figure 3. Plots of eq I for the reactions of OH radicals with ethyl *N,N,N′,N′*-tetramethylphosphorodiamidate (ETMPDA) at 283 ± 1, 297 ± 1 K, 320 ± 1, and 348 ± 1 K, with α-pinene as the reference compound. Experiments were carried out in a ∼4500 L Teflon chamber. The ETMPDA data at 320 ± 1, 297 ± 1, and 283 ± 1 K have been displaced vertically by 0.10, 0.20, and 0.40 units, respectively, for clarity. The solid line through the 297 ± 1 K data is a least-squares fit to the entire data set at that temperature (slope = 3.78 ± 0.17), and the dashed line is a least-squares fit to the data from the first two irradiation periods in each of the four experiments (slope = 4.05 ± 0.14) [the indicated errors are two least-squares standard deviations].

K and, to a lesser extent, 297 ± 1 K are more uncertain, as reflected in part by the larger two-standard deviation errors in Table 1. Replicate postreaction analyses (i.e., after three

dx.doi.org/10.1021/jp407702w | J. Phys. Chem. A 2013, 117, 11038−11048

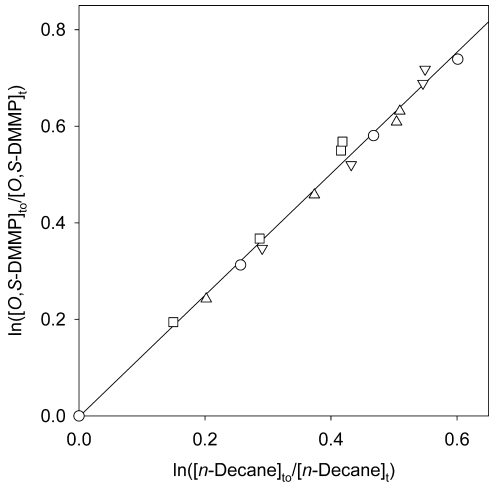

Figure 4. Plot of eq I for the reactions of OH radicals with *O,S*-dimethyl methylphosphonothioate (OSDMMP) at 296 ± 2 K, with *n*-decane as the reference compound. The O_2 contents of the chamber diluent gas were □, 2.1 ± 0.5%; △, 5.8 ± 1.2%; ○, 21% (air); and ▽, 71 ± 3%. Experiments were carried out in a 7220 L Teflon chamber. The solid line is a least-squares fit to the entire data set, with one (0,0) point.

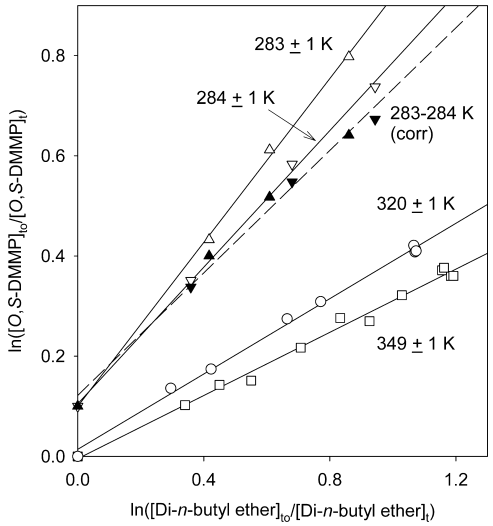

Figure 5. Plots of eq I for the reactions of OH radicals with *O,S*-dimethyl methylphosphonothioate (OSDMMP) at 283 ± 1, 284 ± 1, 320 ± 1, and 349 ± 1 K, with di-*n*-butyl ether as the reference compound. Experiments were carried out in a ∼4500 L Teflon chamber. The experiment at 283 ± 1 K was conducted at or marginally below the local dew point temperature, while that at 284 ± 1 K was conducted well above the local dew point temperature. The OSDMMP data at 283−284 K have been displaced vertically by 0.10 unit for clarity. ▽,△, No correction made for OSDMMP dark decay; ▼, ▲, correction made for OSDMMP dark decay assuming that the OSDMMP dark decay measured postreaction started as soon as the lights were turned on for the first irradiation period (see text).

irradiation periods) for MTMPDA and ETMPDA at these temperatures showed that MTMPDA or ETMPDA decayed faster than the separately measured dark decay rate. This, together with the observation of significant positive intercepts of the least-squares fits to the entire data set at this temperature (see Figure 3), suggests that as the reactions proceeded, MTMPDA or ETMPDA could have been desorbed from the walls and/or aerosol during the irradiation periods (which would lead to a small heating of the Teflon film), followed by a rapid loss of MTMPDA or ETMPDA after the irradiation period. We have therefore used the data points for the first two irradiation periods in each of the four experiments for MTMPDA and ETMPDA at 281.5 ± 1 and 283 ± 1 K, respectively, thereby using data at lower extents of reaction than was the case for the other temperatures studied. For OH + ETMPDA at 297 ± 1 K, where the effect was less pronounced, we have used an average of the slopes obtained from least-squares analyses of the entire data set and from least-squares analysis of the data points from the first two irradiation periods (see Figure 3 and its caption).

For OH + OSDMMP, rate constants were measured at 296 ± 2 K over a range of O_2 content and, as evident from Figure 4, within the experimental uncertainties the rate constant was independent of O_2 content over the range 2.1−71% O_2. Experiments in air were conducted at 349 ± 1, 320 ± 1, and 283−284 K. At room temperature and above, replicate analyses in the dark before and after the reactions showed no evidence for dark decay of OSDMMP, and relative rate plots at 320 ± 1 and 349 ± 1 K are shown in Figure 5. In contrast, while no dark decay of OSDMMP was observed at 283−284 K before reaction, replicate analyses after reaction showed significant dark decays of OSDMMP, of 2.3×10^{-5} s^{-1} in the experiment at 283 ± 1 K and 1.0×10^{-5} s^{-1} in the experiment at 284 ± 1 K. If occurring throughout the reactions, these dark decay rates would be a significant fraction of the measured OSDMMP decays. However, corrections for these dark decays could not be reliably made since they changed during the duration of the experiment. For the experiment at 283 ± 1 K, the chamber temperature was at or slightly below the local dew point temperature during a portion of the experiment (although no condensation on the Teflon film was noticed), while the experiment at 284 ± 1 K was conducted with the chamber temperature above the local dew point temperature. As evident from the relative rate plots in Figure 5, the measured OSDMMP rate constant in the 283 ± 1 K experiment was significantly higher than that in the experiment at 284 ± 1 K, consistent, at least in part, with the faster dark decay after the reaction in the 283 ± 1 K experiment than in that at 284 ± 1 K. If we assume that OSDMMP began to undergo decay to the chamber walls as soon as the first irradiation commenced, then after correcting for OSDMMP decays using the measured postreaction dark decay rates the data for the two experiments are in reasonably good agreement (Figure 5). We have previously reported anomalously high measured OH radical reaction rate constants for DMMP, DMEP, DEMP, DEEP, and TEP when experiments were carried out below the local dew point temperature,[12,14] and this may also be the case for OSDMMP. Given these problems, we use only rate constants for OH + OSDMMP measured at ≥296 K in the derivation of the Arrhenius parameters for OH + OSDMMP.

The rate constant ratios k_1/k_2 obtained by least-squares analyses of the experimental data shown in Figures 2−5 (for temperatures ≥296 K for OSDMMP) are given in Table 1, together with the reference compounds used and, for MTMPDA and ETMPDA, the measured dark decay rates k_3. These rate constant ratios k_1/k_2 are placed on an absolute basis by use of rate constants k_2 of $k_2(\alpha\text{-pinene}) = 1.21 \times 10^{-11}\ e^{436/T}$ cm^3 $molecule^{-1}$ s^{-1},[2] k_2(1,3,5-trimethylbenzene) $= 5.67 \times 10^{-11}$ cm^3 $molecule^{-1}$ s^{-1} at 297 K,[2] k_2(*n*-decane) $= 1.09 \times 10^{-11}$ cm^3 $molecule^{-1}$ s^{-1} at 296 K,[2] and k_2(di-*n*-butyl ether) $= 6.29 \times 10^{-18}\ T^2\ e^{1164/T}$ cm^3 $molecule^{-1}$ s^{-1},[21] and the resulting rate

dx.doi.org/10.1021/jp407702w | J. Phys. Chem. A 2013, 117, 11038−11048

constants k_1 are also given in Table 1. The rate constants measured for OH + MTMPDA at 297 ± 1 K using α-pinene and 1,3,5-trimethylbenzene as the reference compounds agree to within 8%, and the average rate constant for OH + MTMPDA at 297 ± 1 K is (1.73 ± 0.08) × 10^{-10} cm^3 $molecule^{-1}$ s^{-1} (see Figure 2). 1,3,5-Trimethylbenzene could not be used as a reference compound for OH + ETMPDA because ETMPDA was not well resolved from a reaction product of OH + 1,3,5-trimethylbenzene on the GC column used.

The rate constants listed in Table 1 are plotted in Arrhenius form in Figure 6, and the Arrhenius expressions obtained from least-squares analyses of these data are given in Table 2.

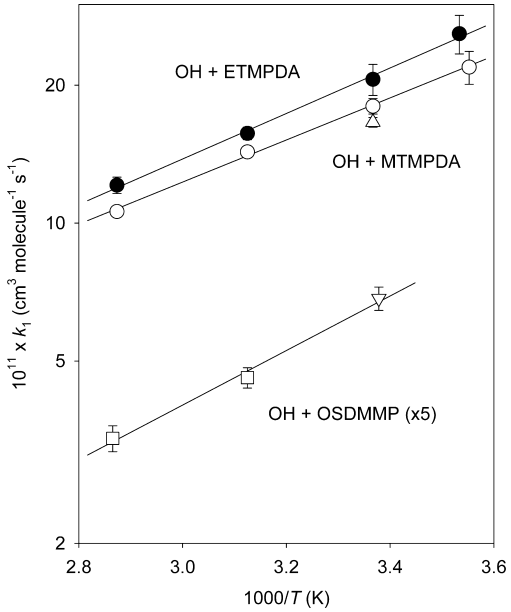

Figure 6. Arrhenius plots of the rate constants k_1 for the reactions of OH radicals with methyl *N,N,N′,N′*-tetramethylphosphorodiamidate (MTMPDA), ethyl *N,N,N′,N′*-tetramethylphosphorodiamidate (ETMPDA), and *O,S*-dimethyl methylphosphonothioate (OSDMMP). The reference compounds used were ○, ●, α-pinene; △, 1,3,5-trimethylbenzene; ▽, *n*-decane; and □, di-*n*-butyl ether. The solid line for OH + MTMPDA is the least-squares fit to the rate constants measured using α-pinene as the reference compound. Note that the rate constants of OSDMMP have been multiplied by a factor of 5 for clarity.

Product Analyses by API-MS. *NO_3 + MTMPDA, OH + MTMPDA, and OH + ETMPDA.* For these reactions, the positive ion API-MS and API-MS/MS spectra were significantly easier to interpret than the negative ion spectra and provided the most unambiguous and useful information. In positive ion mode, prior to reaction, intense ion peaks at *m/z* 167 and 333 were observed from the NO_3 + MTMPDA and OH + MTMPDA reactions, and at *m/z* 181 and 361 from the OH + ETMPDA reaction, these being attributed to protonated MTMPDA or ETMPDA and the protonated MTMPDA or ETMPDA dimer, respectively. In each reaction, a weaker ion peak at *m/z* 185 ($[MTMPDA+H+H_2O]^+$) or *m/z* 199 ($[ETMPDA+H+H_2O]^+$) was also observed. After reaction, additional weak ion peaks were observed (Figure 7), at *m/z* 181 and 347 in the MTMPDA reactions and at *m/z* 195 and 375 in the OH + ETMPDA reaction. These ions are attributed to the presence of a product of molecular weight 180 (MTMPDA reactions) or 194 (OH + ETMPDA reaction), respectively (see the caption to Figure 7 for the peak assignments). The OH + ETMPDA reaction also showed the presence of ion peaks at *m/z* 167 and 347, and these are attributed to the presence of a molecular weight 166 product, which may be a second-generation product. On the basis of arguments similar to those made for the OH + $(CH_3O)_2P(O)N(CH_3)_2$ reaction previously,[15] the molecular weight 180 and 194 products are attributed to $CH_3OP(O)[N(CH_3)_2]N(CH_3)CHO$ and $C_2H_5OP(O)[N(CH_3)_2]N(CH_3)CHO$, respectively, which are expected to be observed by API-MS in positive ion mode and also by gas chromatography (see below).

The negative ion mode API-MS and API-MS/MS spectra were much more difficult to unambiguously interpret. Several of the product ions from the NO_3 + MTMPDA, OH + MTMDA and OH + ETMPDA reactions were observed at the same masses and were consistent with the presence of products of molecular weight 166, 180, and possibly 212 from NO_3 + MTMPDA, 166 and/or 180 from OH + MTMPDA, and 166, 180, and 194 from OH + ETMPDA. It is possible that the molecular weight 180 and 194 products attributed to $CH_3OP(O)[N(CH_3)_2]N(CH_3)CHO$ and $C_2H_5OP(O)[N(CH_3)_2]N(CH_3)CHO$ from the MTMPDA and ETMPDA reactions, respectively, were also observed in negative ion mode. It is also possible that the molecular weight 180 product tentatively observed in negative ion mode from MTMPDA is $HC(O)OP(O)[N(CH_3)_2]_2$, while a molecular weight 166 product from both reactions would presumably imply a second generation product such as $HOP(O)[N(CH_3)_2]N(CH_3)CHO$.

OH + OSDMMP. In positive ion mode, no new ion peaks were observed after reaction. However, product ion peaks were observed after reaction in negative ion mode, as shown by the API-MS spectrum in Figure 8, and their assignments are given in the caption to Figure 8, based on API-MS/MS spectra of the ion peaks at *m/z* 125, 156, 170, 172, 188, 205, 219, 235, 252, 261, 266, 280, 281, 282, and 298. While the identities of some of the observed ion peaks are uncertain, the presence of products of molecular weight 110, 126, and 142 was indicated, noting that the evidence for formation of a molecular weight 142 product was less certain and that one or more of these products could have arisen, at least in part, from the reaction of the 10% impurity of molecular weight 156. On the basis of postulated mechanisms for the reactions of OH radicals with alkyl phosphates, phosphonates, and phosphorothioates,[8,10,15,18] potential products from OH + OSDMMP include $CH_3SP(O)(CH_3)OH$ (mw 126), $CH_3OP(O)(CH_3)SH$ (mw 126), $CH_3OP(S)(CH_3)OH$ (mw 126), and $CH_3OP(O)(CH_3)OH$ (mw 110). It is possible that the molecular weight 142 product is $CH_3SP(S)(CH_3)OH$ and/or $CH_3SP(O)(CH_3)SH$ arising from the reaction of OH radicals with the molecular weight 156 impurity attributed to $(CH_3S)_2P(O)CH_3$.

Analyses by Gas Chromatography. GC-FID analyses of reacted NO_3 + MTMPDA and OH + MTMPDA mixtures showed the presence of a single product from each reaction with identical GC retention times and which GC−MS analysis showed to be of molecular weight 180. Likewise, GC-FID analyses of reacted OH + ETMPDA mixtures showed the presence of a product that GC−MS analyses showed to be of molecular weight 194. In our API-MS analyses of the NO_3 + MTMPDA, OH + MTMPDA, and OH + ETMPDA reactions (see above), ion peaks observed in positive ion mode suggested the formation of products of these same molecular weights. The molecular weights of these products indicate that for both

dx.doi.org/10.1021/jp407702w | J. Phys. Chem. A 2013, 117, 11038−11048

Table 2. Arrhenius Parameters ($k = Ae^{-B/T}$) for the Reactions of OH Radicals with MTMPDA, ETMPDA, and OSDMMP, Together with Literature Arrhenius Parameters for Related Compounds

organophosphorus compound[a]	$10^{12} \times A$ (cm^3 $molecule^{-1}$ s^{-1})	B (K)[b]	$10^{11} \times k$ (298 K)[c] (cm^3 $molecule^{-1}$ s^{-1})	ref
MTMPDA	4.96[d]	−1058 ± 71[d]	17.3	this work
ETMPDA	4.46	−1144 ± 95	20.7	this work
OSDMMP	0.131	−1370 ± 229	1.30	this work
DMDMPDA	0.605	−1185 ± 144	3.23	15
DMHP	1.01	−474 ± 159	0.497	14
DMMP	0.0625	−1538 ± 112	1.09	14
DMEP	0.0903	−1539 ± 27	1.58	14
DEMP	0.435	−1444 ± 148	5.53	14
DEEP	0.408	−1485 ± 328	5.95	14
TEP	0.407	−1448 ± 145	5.25	14
IMMP	0.272	−1642 ± 144	6.72	15

[a]DMDMPA = $(CH_3O)_2P(O)N(CH_3)_2$; DMHP = $(CH_3O)_2P(O)H$; DMMP = $(CH_3O)_2P(O)CH_3$; DMEP = $(CH_3O)_2P(O)C_2H_5$; DEMP = $(C_2H_5O)_2P(O)CH_3$; DEEP = $(C_2H_5O)_2P(O)C_2H_5$; TEP = $(C_2H_5O)_3PO$; and IMMP = $(CH_3)_2CHOP(O)(CH_3)OCH_3$. [b]The cited errors are two least-squares standard deviations from Arrhenius plots such as those shown in Figure 6. The estimated overall uncertainties in the values of B are ±300 K, except for OSDMMP and DEEP for which they are ±400 K. [c]The estimated overall uncertainties in the 298 K rate constants are ±12%, except for MTMPDA, ETMPDA, and DEEP for which they are ±15%. [d]The temperature dependence B was obtained from a least-squares analyses of the rate constants measured over the temperature range 281.5−348 K using α-pinene as the reference compound (Figure 6). Since the 297 ± 1 K rate constant obtained using both α-pinene and 1,3,5-trimethylbenzene was 3.5% lower than that obtained using only α-pinene as the reference compound (Table 1), the pre-exponential factor A from the least-squares analysis of the rate constants measured over the temperature range 281.5−348 K using α-pinene as the reference compound has been decreased by 3.5%.

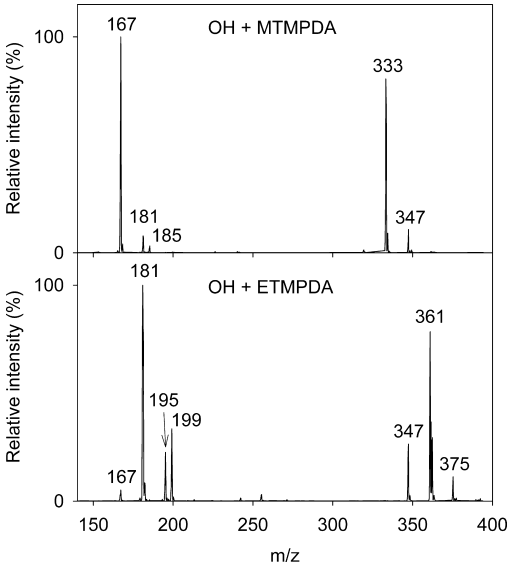

Figure 7. Positive ion API-MS analysis of CH_3ONO−NO−air irradiations of (top) methyl *N,N,N′,N′*-tetramethylphosphorodiamidate (MTMPDA) and (bottom) ethyl *N,N,N′,N′*-tetramethylphosphorodiamidate (ETMPDA). On the basis of API-MS/MS analyses, products observed had molecular weights of 180 from OH + MTMPDA and 166 and 194 from OH + ETMPDA. The peak assignments are: for OH + MTMPDA, m/z 167, $[MTMPDA + H]^+$; m/z 181, $[180 + H]^+$; m/z 185, $[MTMPDA + H + H_2O]^+$; m/z 333, $[MTMPDA + MTMPDA + H]^+$; and m/z 347, $[MTMPDA + 180 + H]^+$; and for OH + ETMPDA, m/z 167, $[166 + H]^+$; m/z 181, $[ETMPDA + H]^+$; m/z 195, $[194 + H]^+$; m/z 199, $[ETMPDA + H + H_2O]^+$; m/z 347, $[ETMPDA + 166 + H]^+$; m/z 361, $[ETMPDA + ETMPDA + H]^+$; and m/z 375, $[ETMPDA + 194 + H]^+$. The molecular weight 166 product from OH + ETMPDA may be a second-generation product.

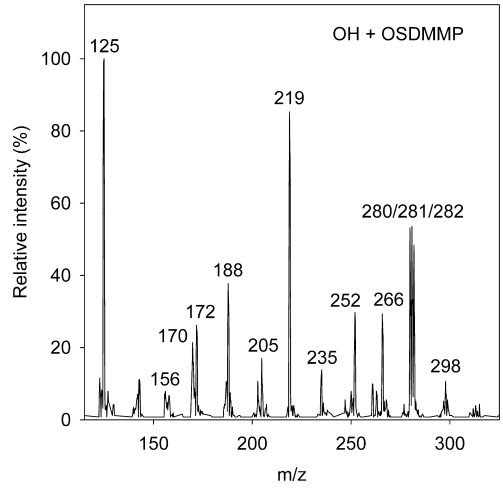

Figure 8. Negative ion API-MS analysis of an irradiated CH_3ONO−NO−*O,S*-dimethyl methylphosphonothioate (OSDMMP)−air mixture. On the basis of API-MS/MS analyses, products observed had molecular weights of 110, 126, and 142. The peak assignments are: m/z 125, $[126 - H]^-$; m/z 156, $[110 + NO_2]^-$; m/z 170, $[110 + 60]^-$; m/z 172, $[126 + NO_2]^-$ and $[110 + NO_3]^-$; m/z 188, $[126 + NO_3]^-$ and $[142 + NO_2]^-$; m/z 205, $[110 + 95]^-$ and/or $[142 + 63]^-$; m/z 219, $[110 + 110 - H]^-$; m/z 235, $[110 + 126 - H]^-$; m/z 252, $[110 + 110 + O_2]^-$; m/z 266, $[110 + 110 + NO_2]^-$; m/z 280, $[110 + 110 + 60]^-$; m/z 281, $[110 + 110 + 61]^-$; m/z 282, $[110 + 110 + NO_3]^-$; and m/z 298, $[126 + 110 + NO_3]^-$ and $[126 + 126 + NO_2]^-$.

MTMPDA and ETMPDA, they are formed by converting a CH_3 group into a CHO group. H-atom abstraction from OCH_3 and OC_2H_5 groups attached to the P-atom appears to generally result in the replacement of OCH_3 and OC_2H_5 by OH (i.e., >P(O)OR → >P(O)OH, where R = CH_3 or C_2H_5),[8,10] and in our API-MS analyses these >P(O)OH products are readily observed in negative ion mode, but not in positive ion mode.[8,10] Moreover, these >P(O)OH products do not elute from GC columns under our conditions.[8,10] The molecular weight 180 product from the NO_3 + MTMPDA and OH + MTMPDA reactions is therefore attributed to $CH_3OP(O)[N(CH_3)_2]N(CH_3)CHO$, and the molecular weight 194 product from OH + MTMPDA is attributed to $C_2H_5OP(O)[N(CH_3)_2]N(CH_3)CHO$.

dx.doi.org/10.1021/jp407702w | J. Phys. Chem. A 2013, 117, 11038−11048

Authentic standards of $CH_3OP(O)[N(CH_3)_2]N(CH_3)CHO$ and $C_2H_5OP(O)[N(CH_3)_2]N(CH_3)CHO$ were not available, and hence the Effective Carbon Number (ECN) concept[22] was used to estimate their GC-FID responses relative to those of MTMPDA and ETMPDA, respectively. FID detectors respond to carbon, and in alkanes, each carbon atom contributes 1.00 toward the ECN.[22] Some heteroatom-containing groups have lower responses, with CHO groups having zero response.[22] Because −CHO groups have a zero FID response,[22] we assumed that the ECN of $CH_3OP(O)[N(CH_3)_2]N(CH_3)CHO$ relative to that of MTMPDA was 0.80 (4.0/5.0) and that the ECN of $C_2H_5OP(O)[N(CH_3)_2]N(CH_3)CHO$ relative to that of ETMPDA was 0.83 (5.0/6.0).

A plot of the GC-FID area counts of $CH_3OP(O)[N(CH_3)_2]N(CH_3)CHO$ formed against the area counts of MTMPDA lost during NO_3 + MTMPDA reactions was a reasonable straight line with a close to zero intercept (Figure S1 in the Supporting Information). This suggests that $CH_3OP(O)[N(CH_3)_2]N(CH_3)CHO$ is significantly less reactive than MTMPDA toward NO_3 radicals. After correction for the small differences in estimated ECNs (see above) and for the amount of MTMPDA lost by dark decay, a least-squares analysis of the data shown in Figure S1, Supporting Information, leads to a $CH_3OP(O)[N(CH_3)_2]N(CH_3)CHO$ molar formation yield from NO_3 + MTMPDA of ∼25%. In the OH radical reactions of MTMPDA and ETMPDA, plots of the GC-FID area counts of $CH_3OP(O)[N(CH_3)_2]N(CH_3)CHO$ or $C_2H_5OP(O)[N(CH_3)_2]N(CH_3)CHO$ formed against the area counts of MTMPDA or ETMPDA lost resulted in slopes that decreased with increasing extent of reaction. This indicates losses of $CH_3OP(O)[N(CH_3)_2]N(CH_3)CHO$ or $C_2H_5OP(O)[N(CH_3)_2]N(CH_3)CHO$ during these reactions, by reaction with OH radicals as well as dark decays (which were an order of magnitude faster than the dark decays of MTMPDA or ETMPDA and most rapid at the lowest temperatures studied). We therefore linearized plots of $CH_3OP(O)[N(CH_3)_2]N(CH_3)CHO$ or $C_2H_5OP(O)[N(CH_3)_2]N(CH_3)CHO$ formed (after correction for their losses) against the amounts of MTMPDA or ETMPDA reacted, by varying the ratio (loss rate of $CH_3OP(O)[N(CH_3)_2]N(CH_3)CHO$ or $C_2H_5OP(O)[N(CH_3)_2]N(CH_3)CHO$)/(loss rate of MTMPDA or ETMPDA) = $k_{prod}/k_{reactant}$. Thus, if the value of $k_{prod}/k_{reactant}$ used was too low, then the slope of the plot decreased with extent of reaction and a least-squares analysis yielded a positive intercept; if the value of $k_{prod}/k_{reactant}$ used was too high, then the slope of the plot increased with the extent of reaction and a least-squares analysis yielded a negative intercept. The linearized plots are shown in Figures S2 (OH + MTMPDA) and S3 (OH + ETMPDA), Supporting Information. After correction for the small differences in estimated ECNs (see above) and for the amounts of MTMPDA or ETMPDA lost by dark decay, the formation yields and rate ratios $k_{prod}/k_{reactant}$ derived were: for formation of $CH_3OP(O)[N(CH_3)_2]N(CH_3)CHO$ from OH + MTMPDA, 14% and 0.9 at 281.5 ± 1 K; 16% and 0.45 at 297 ± 1 K; 12% and 0.45 at 320 ± 1 K; and 11% and 0.45 at 348 ± 1 K; and for formation of $C_2H_5OP(O)[N(CH_3)_2]N(CH_3)CHO$ from OH + ETMPDA, 11% and 0.6 at 283 ± 1 K; 14% and 0.5 at 297 ± 1 K; 10% and 0.4 at 320 ± 1 K; and 9.5% and 0.4 at 348 ± 1 K. For both the OH + MTMPDA and OH + ETMPDA reactions, the rate ratios and formation yields at 320 ± 1 and 348 ± 1 K were more uncertain due to the lesser amounts of data obtained. The observed more rapid dark decays of $CH_3OP(O)[N(CH_3)_2]N(CH_3)CHO$ and $C_2H_5OP(O)[N(CH_3)_2]N(CH_3)CHO$ at 281−283 K than at the higher temperatures may explain the higher derived rate ratios at these temperatures compared to those at the other temperatures. No products were observed from GC-FID analyses of OH + OSDMMP.

Aerosol formation, as measured using a TSI 3936L72 scanning mobility particle sizer, showed that in an irradiated CH_3ONO−NO−MTMPDA−air mixture, after 60% consumption of the initial 1.5×10^{13} molecules cm^{-3} of MTMPDA, the aerosol yield (defined as aerosol formed/MTMPDA consumed, assuming equal densities of MTMPDA and aerosol and correcting for wall losses of the aerosol) was ∼55%. The corresponding aerosol yield in an NO_3 + MTMPDA reaction was ∼15%.

DISCUSSION

MTMPDA and ETMPDA. As for other alkyl phosphates, alkyl phosphonates, and alkyl phosphoroamidates,[8,10,15] any reaction of MTMPDA with O_3 is slow. However, in contrast to dimethyl *N*,*N*-dimethylphosphoroamidate $[(CH_3O)_2P(O)N(CH_3)_2$; DMDMPA] for which an upper limit to the room temperature rate constant for reaction with NO_3 radicals of $<3.9 \times 10^{-14}$ cm^3 $molecule^{-1}$ s^{-1} has been measured,[5] MTMPDA reacts rapidly with NO_3 radicals, and ETMPDA is expected to be at least as reactive as MTMPDA with respect to reaction with NO_3 radicals.

The reactions of OH radicals with MTMPDA and ETMPDA exhibit a significant negative temperature dependence ($B \approx -1100$ K), somewhat less negative than those for the reactions of OH radicals with DMMP, DMEP, DEMP, and DEEP for which $B \approx -1500$ K (Table 2), but similar to that for DMDMPA (Table 2).[15] By analogy with the reactions of OH radicals with alkyl phosphates, alkyl phosphonates, and DMDMPA,[8,10,15,19,20] the reactions are likely to occur by initial complex formation followed by decomposition involving C−H bond breakage. For MTMPDA and ETMPDA, there are two expected pathways in each case, involving H-atom abstraction from the $-OCH_3$ or $-OC_2H_5$ group and H-atom abstraction from the $-CH_3$ groups in the $-N(CH_3)_2$ moieties. For example, for MTMPDA:

$$OH + CH_3OP(O)[N(CH_3)_2]_2 \leftrightarrow [complex] \rightarrow H_2O + {}^{\bullet}CH_2OP(O)[N(CH_3)_2]_2 \quad (4a)$$

$$OH + CH_3OP(O)[N(CH_3)_2]_2 \leftrightarrow [complex] \rightarrow H_2O + CH_3OP(O)[N(CH_3)_2]N(CH_3)C^{\bullet}H_2 \quad (4b)$$

Subsequent reactions of the $CH_3OP(O)[N(CH_3)_2]N(CH_3)C^{\bullet}H_2$ radical are expected to lead to formation of $CH_3OP(O)[N(CH_3)_2]N(CH_3)CHO$.

$$CH_3OP(O)[N(CH_3)_2]N(CH_3)C^{\bullet}H_2 + O_2 \rightarrow CH_3OP(O)[N(CH_3)_2]N(CH_3)CH_2OO^{\bullet} \quad (5)$$

$$CH_3OP(O)[N(CH_3)_2]N(CH_3)CH_2OO^{\bullet} + NO \rightarrow CH_3OP(O)[N(CH_3)_2]N(CH_3)CH_2O^{\bullet} + NO_2 \quad (6)$$

$$CH_3OP(O)[N(CH_3)_2]N(CH_3)CH_2O^{\bullet} + O_2 \rightarrow CH_3OP(O)[N(CH_3)_2]N(CH_3)CHO + HO_2 \quad (7)$$

dx.doi.org/10.1021/jp407702w | J. Phys. Chem. A 2013, 117, 11038−11048

The observation that the room temperature rate constant for OH + MTMPDA is a factor of 5−6 higher than that for OH + $(CH_3O)_2P(O)N(CH_3)_2$ (Table 2) suggests that the majority of the OH + MTMPDA reaction proceeds by H-atom abstraction from the C−H bonds in the $N(CH_3)_2$ groups. Furthermore, replacing a OCH_3 group in MTMPDA by a OC_2H_5 group in ETMPDA increases the room temperature rate constant by 2.7×10^{-11} cm^3 $molecule^{-1}$ s^{-1} (Table 1, using rate constants measured with α-pinene as the reference compound). Since replacing two OCH_3 groups in DMMP or DMEP by two OC_2H_5 groups in DEMP or DEEP, respectively, increases the room temperature rate constants by 4.4×10^{-11} cm^3 $molecule^{-1}$ s^{-1} (Table 2), it appears that the reactivity of the OCH_3 and OC_2H_5 groups in MTMPDA and ETMPDA are similar to those in DMMP, DMEP, DEMP, and DEEP and that the partial rate constants for H-atom abstraction by OH radicals from the OCH_3 and OC_2H_5 groups in MTMPDA and ETMPDA are $\sim 6 \times 10^{-12}$ cm^3 $molecule^{-1}$ s^{-1} and $\sim 3 \times 10^{-11}$ cm^3 $molecule^{-1}$ s^{-1}, respectively, at 298 K. This implies that H-atom abstraction from the OCH_3 and OC_2H_5 groups in MTMPDA and ETMPDA accounts for ∼3% and ∼15% of the overall reactions, respectively, with the remainder of the reactions proceeding by H-atom abstraction from the C−H bonds in the $N(CH_3)_2$ groups. Our measured formation yields of the products attributed to $CH_3OP(O)[N(CH_3)_2]N(CH_3)$-CHO and $C_2H_5OP(O)[N(CH_3)_2]N(CH_3)CHO$ from the OH + MTMPDA and OH + ETMPDA reactions, respectively, of ∼14% and ∼11% therefore account for only a small fraction of the reaction pathways proceeding by H-atom abstraction from the $N(CH_3)_2$ groups.

OH + OSDMMP. As for DMMP $[(CH_3O)_2P(O)$-$CH_3]$,[10,19,20] the reaction of OH radicals with OSDMMP is expected to proceed by H-atom abstraction from the C−H bonds of the OCH_3 and SCH_3 groups, with H-atom abstraction from the CH_3 group being minor.

$$OH + CH_3SP(O)(CH_3)OCH_3 \rightarrow H_2O + CH_3SP(O)(CH_3)OC^{\bullet}H_2 \quad (8a)$$

$$OH + CH_3SP(O)(CH_3)OCH_3 \rightarrow H_2O + C^{\bullet}H_2SP(O)(CH_3)OCH_3 \quad (8b)$$

In addition, by analogy with OH + dimethyl sulfide,[23−25] it is possible that a pathway involving OH radical addition to the S-atom to form an OH-OSDMMP adduct, which can back-decompose to reactants or react with O_2 to form products, also occurs.

$$OH + CH_3SP(O)(CH_3)OCH_3(+M) \rightarrow CH_3S(OH)P(O)(CH_3)OCH_3(+M) \quad (9)$$

$$CH_3S(OH)P(O)(CH_3)OCH_3(+M) \rightarrow OH + CH_3SP(O)(CH_3)OCH_3(+M) \quad (10)$$

$$CH_3S(OH)P(O)(CH_3)OCH_3 + O_2 \rightarrow \text{products, including } CH_3S(O)P(O)(CH_3)OCH_3 \quad (11)$$

The independence of the measured rate constant at 296 ± 2 K over the range 2.1−71% O_2, and the lack of any evidence for products arising from the OH radical addition channel in our API-MS analyses, suggest that at 296 K the reaction of OH radicals with OSDMMP proceeds only by H-atom abstraction. The negative temperature dependence measured here for OH + OSDMMP over the range 296−349 K is similar in magnitude to those for other alkyl phosphates and phosphonates (Table 2).

For OH + dimethyl sulfide, the stability of the $CH_3S(OH)$-CH_3 adduct is ∼11 kcal mol^{-1},[25] and in air the OH radical addition channel becomes evident below ∼310 K.[23,24] Our kinetic data for OH + OSDMMP at 283−284 K, if the correction for the observed postreaction OSDMMP dark decay is applied from the time that the reaction was initiated, are within ∼13% of the rate constant predicted from extrapolation of the 296−349 K data, suggesting that at 283−284 K and atmospheric pressure of air the OH radical addition pathway [reactions 9 through 11] is, at most, minor. This then suggests that any $CH_3S(OH)P(O)(CH_3)OCH_3$ adduct is less stable toward back-decomposition to reactants than is the CH_3S-$(OH)CH_3$ adduct, with the stability of the $CH_3S(OH)P(O)$-$(CH_3)OCH_3$ adduct being ≤10 kcal mol^{-1} assuming that the rate constants for reactions 9 and 11 are similar to those for the corresponding reactions in the OH + dimethyl sulfide system.

In order to explain the observed products from the reactions of OH radicals with DMMP and TEP,[8,10] it has previously been proposed[8,10] that the intermediate alkoxy radicals of structure $>P(O)OCH(O^{\bullet})R$ (R = H or CH_3), formed after initial H-atom abstraction from OCH_3 or OC_2H_5 groups, can isomerize via a 5-membered ring to form $>P(OH)=O$ + $RC^{\bullet}O$ (see Scheme 1). In the case of OSDMMP, such a reaction sequence

Scheme 1

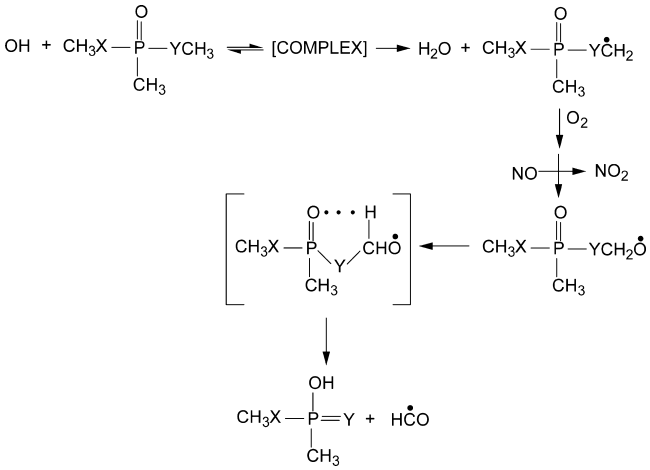

(Scheme 1) would lead to formation of the first-generation phosphorus-containing products $CH_3SP(O)(CH_3)OH$ [X = S and Y = O] and $CH_3OP(S)(CH_3)OH$ [X = O and Y = S], both of molecular weight 126. On the basis of kinetic data for organophosphorus compounds of structure $(CH_3O)_nP(O)$-$(SCH_3)_{3-n}$ and $(CH_3O)_nP(S)(SCH_3)_{3-n}$,[3,4] it is anticipated that $CH_3OP(S)(CH_3)OH$ will be significantly more reactive than $CH_3SP(O)(CH_3)OH$ toward OH radicals (because of the presence of a P=S bond, with, for example, $(CH_3O)_3PS$ being a factor of ∼10 more reactive than $(CH_3O)_3PO$). Since the reactions of OH radicals with $(CH_3O)_3PS$, $(CH_3O)_2P(S)$-SCH_3, $(C_2H_5O)_3PS$, and $(C_2H_5O)_2P(S)CH_3$ lead to the formation of $(CH_3O)_3PO$ (in 28 ± 4% yield),[26] $(CH_3O)_2P$-$(O)SCH_3$ (in 13 ± 5% yield),[26] $(C_2H_5O)_3PO$ (in 60 ± 12% yield),[18] and $(C_2H_5O)_2P(O)CH_3$ (in 21 ± 4% yield),[13]

dx.doi.org/10.1021/jp407702w | J. Phys. Chem. A 2013, 117, 11038−11048

respectively, $CH_3OP(O)(CH_3)OH$ (molecular weight 110) is therefore an expected second-generation product from OH + OSDMMP, being formed from OH + $CH_3OP(S)(CH_3)OH$. The proposed reaction mechanism therefore accounts for the molecular weight products observed in our API-MS analyses.

CONCLUSIONS AND ATMOSPHERIC IMPLICATIONS

Combining our OH and NO_3 radical rate constants with an assumed 12 h average daytime OH radical concentration of 2×10^6 molecules cm^{-3} and an average 12 h nighttime NO_3 radical concentration of 5×10^8 molecules cm^{-3} leads to calculated lifetimes of MTMPDA and ETMPDA of ~45 min during daytime and (for MTMPDA) ~25 min during nighttime. The corresponding lifetime for OSDMMP due to daytime reaction with OH radicals is calculated to be 11 h. On the basis of our present and previous[4,8,10,15] studies, the reactions of MTMPDA and ETMPDA with O_3 and of OSDMMP with NO_3 radicals and O_3 will of no importance under atmospheric conditions. The products observed from OH and NO_3 + MTMPDA and from OH + ETMPDA were attributed to $CH_3OP(O)[N(CH_3)_2]N(CH_3)CHO$ and $C_2H_5OP(O)[N(CH_3)_2]N(CH_3)CHO$, respectively, and products with molecular weights consistent with $CH_3SP(O)(CH_3)OH$, $CH_3OP(S)(CH_3)OH$, and $CH_3OP(O)(CH_3)OH$ were observed from OH + OSDMMP.

ASSOCIATED CONTENT

Supporting Information

Plots of GC-FID area counts of products formed against MTMPDA or ETMPDA lost for NO_3 + MTMPDA, OH + MTMPDA and OH + ETMPDA. This material is available free of charge via the Internet at http://pubs.acs.org.

AUTHOR INFORMATION

Corresponding Author

*(R.A.) E-mail: ratkins@mail.ucr.edu. Tel: (951) 827-4191.

Notes

The authors declare no competing financial interest.

ACKNOWLEDGMENTS

This work was supported by ENSCO, Inc. While this research has been funded by this agency, the results and content of this publication do not necessarily reflect the views and opinions of the funding agency.

REFERENCES

(1) Worthing, C. R., Hance, R. J., Eds. *The Pesticide Manual*, 9th ed.; British Crop Protection Council: Farnham, U.K., 1991.

(2) Atkinson, R.; Arey, J. Atmospheric Degradation of Volatile Organic Compounds. *Chem. Rev.* **2003**, *103*, 4605−4638.

(3) Tuazon, E. C.; Atkinson, R.; Aschmann, S. M.; Arey, J.; Winer, A. M.; Pitts, J. N., Jr. Atmospheric Loss Processes of 1,2-Dibromo-3-chloropropane and Trimethyl Phosphate. *Environ. Sci. Technol.* **1986**, *20*, 1043−1046.

(4) Goodman, M. A.; Aschmann, S. M.; Atkinson, R.; Winer, A. M. Kinetics of the Atmospherically Important Gas-Phase Reactions of a Series of Trimethyl Phosphorothioates. *Arch. Environ. Contam. Toxicol.* **1988**, *17*, 281−288.

(5) Goodman, M. A.; Aschmann, S. M.; Atkinson, R.; Winer, A. M. Atmospheric Reactions of a Series of Dimethyl Phosphoroamidates and Dimethyl Phosphorothioamidates. *Environ. Sci. Technol.* **1988**, *22*, 578−583.

(6) Atkinson, R.; Aschmann, S. M.; Goodman, M. A.; Winer, A. M. Kinetics of the Gas-Phase Reactions of the OH Radical with $(C_2H_5)_3PO$ and $(CH_3O)_2P(S)Cl$ at 296 ± 2 K. *Int. J. Chem. Kinet.* **1988**, *20*, 273−281.

(7) Martin, P.; Tuazon, E. C.; Atkinson, R.; Maughan, A. D. Atmospheric Gas-Phase Reactions of Selected Phosphorus-Containing Compounds. *J. Phys. Chem. A* **2002**, *106*, 1542−1550.

(8) Aschmann, S. M.; Tuazon, E. C.; Atkinson, R. Atmospheric Chemistry of Diethyl Methylphosphonate, Diethyl Ethylphosphonate, and Triethyl Phosphate. *J. Phys. Chem. A* **2005**, *109*, 2282−2291.

(9) Sun, F.; Zhu, T.; Shang, J.; Han, L. Gas-Phase Reaction of Dichlorvos, Carbaryl, Chlordimeform, and 2,4-D Butyl Ester with OH Radicals. *Int. J. Chem. Kinet.* **2005**, *37*, 755−762.

(10) Aschmann, S. M.; Tuazon, E. C.; Atkinson, R. Atmospheric Chemistry of Dimethyl Phosphonate, Dimethyl Methylphosphonate, and Dimethyl Ethylphosphonate. *J. Phys. Chem. A* **2005**, *109*, 11828−11836.

(11) Feigenbrugel, V.; Le Person, A.; Le Calvé, S.; Mellouki, A.; Muñoz, A.; Wirtz, K. Atmospheric Fate of Dichlorvos: Photolysis and OH-Initiated Oxidation Studies. *Environ. Sci. Technol.* **2006**, *40*, 850−857.

(12) Aschmann, S. M.; Long, W. D.; Atkinson, R. Temperature-Dependent Rate Constants for the Gas-Phase Reactions of OH Radicals with 1,3,5-Trimethylbenzene, Triethyl Phosphate, and a Series of Alkylphosphonates. *J. Phys. Chem. A* **2006**, *110*, 7393−7400.

(13) Aschmann, S. M.; Atkinson, R. Kinetic and Product Study of the Gas-Phase Reactions of OH Radicals, NO_3 Radicals, and O_3 with $(C_2H_5O)_2P(S)CH_3$ and $(C_2H_5O)_3PS$. *J. Phys. Chem. A* **2006**, *110*, 13029−13035.

(14) Aschmann, S. M.; Long, W. D.; Atkinson, R. Rate Constants for the Gas-Phase Reactions of OH Radicals with Dimethyl Phosphonate over the Temperature Range of 278−351 K and for a Series of Other Organophosphorus Compounds at ~280 K. *J. Phys. Chem. A* **2008**, *112*, 4793−4799.

(15) Aschmann, S. M.; Tuazon, E. C.; Long, W. D.; Atkinson, R. Atmospheric Chemistry of Isopropyl Methyl Methylphosphonate and Dimethyl *N*,*N*-Dimethylphosphoroamidate. *J. Phys. Chem. A* **2010**, *114*, 3523−3532.

(16) Aschmann, S. M.; Tuazon, E. C.; Long, W. D.; Atkinson, R. Atmospheric Chemistry of Dichlorvos. *J. Phys. Chem. A* **2011**, *115*, 2756−2764.

(17) Muñoz, A.; Vera, T.; Sidebottom, H.; Mellouki, A.; Borrás, E.; Ródenas, M.; Clemente, E.; Vázquez, M. Studies on the Atmospheric Degradation of Chlorpyrifos-Methyl. *Environ. Sci. Technol.* **2011**, *45*, 1880−1886.

(18) Tuazon, E. C.; Aschmann, S. M.; Atkinson, R. Products of the Gas-Phase Reactions of OH Radicals with $(C_2H_5O)_2P(S)CH_3$ and $(C_2H_5O)_3PS$. *J. Phys. Chem. A* **2007**, *111*, 916−924.

(19) Cory, M. G.; Taylor, D. E.; Bunte, S. W.; Runge, K.; Vasey, J. L.; Burns, D. S. Theoretical Methodology for Prediction of Tropospheric Oxidation of Dimethyl Phosphonate and Dimethyl Methylphosphonate. *J. Phys. Chem. A* **2011**, *115*, 1946−1954.

(20) Burns, D. S.; Cory, M. G.; Taylor, D. E.; Bunte, S. W.; Runge, K.; Vasey, J. L. A Comparison of Primary and Secondary Hydrogen Abstraction from Organophosphates by Hydroxyl Radical. *Int. J. Chem. Kinet.* **2013**, *45*, 187−201.

(21) Mellouki, A.; Teton, S.; Le Bras, G. Kinetics of OH Radical Reactions with a Series of Ethers. *Int. J. Chem. Kinet.* **1995**, *27*, 791−805.

(22) Scanlon, J. T.; Willis, D. E. Calculation of Flame Ionization Detector Relative Response Factors Using the Effective Carbon Number Concept. *J. Chromat. Sci.* **1985**, *23*, 333−340.

(23) Hynes, A. J.; Wine, P. H. Direct Kinetic and Mechanistic Study of the OH-Dimethyl Sulfide Reaction under Atmospheric Conditions. In *The Chemistry of Acid Rain: Sources and Atmospheric Processes*, ACS Symposium Series No. 349; Johnson, R. W., Gordon, G. E., Eds.; American Chemical Society: Washington, DC, 1987; pp 133−141.

(24) Albu, M.; Barnes, I.; Becker, K. H.; Patroescu-Klotz, I.; Mocanu, R.; Benter, T. Rate Coefficients for the Gas-Phase Reaction of OH

Radicals with Dimethyl Sulfide: Temperature and O_2 Partial Pressure Dependence. *Phys. Chem. Chem. Phys.* **2006**, *8*, 728−736.
(25) Williams, M. B.; Campuzano-Jost, P.; Cossairt, B. M.; Hynes, A. J.; Pounds, A. J. Experimental and Theoretical Studies of the Reaction of OH Radical with Alkyl Sulfides: 1. Direct Observations of the Formation of the OH-DMS Adduct - Pressure Dependence of the Forward Rate of Addition and Development of a Predictive Expression at Low Temperature. *J. Phys. Chem. A* **2007**, *111*, 89−104.
(26) Atkinson, R.; Aschmann, S. M.; Arey, J.; McElroy, P. A.; Winer, A. M. Product Formation from the Gas-Phase Reactions of the OH Radical with $(CH_3O)_3PS$ and $(CH_3O)_2P(S)SCH_3$. *Environ. Sci. Technol.* **1989**, *23*, 243−244.

Supporting Information

for

Atmospheric Chemistry of Methyl- and Ethyl *N,N,N′,N′*-tetramethylphosphorodiamidate and *O,S*-Dimethyl methylphosphonothioate

Sara M. Aschmann and Roger Atkinson*

Air Pollution Research Center

University of California

Riverside, CA 92521

Pages: 4

Figures: 3

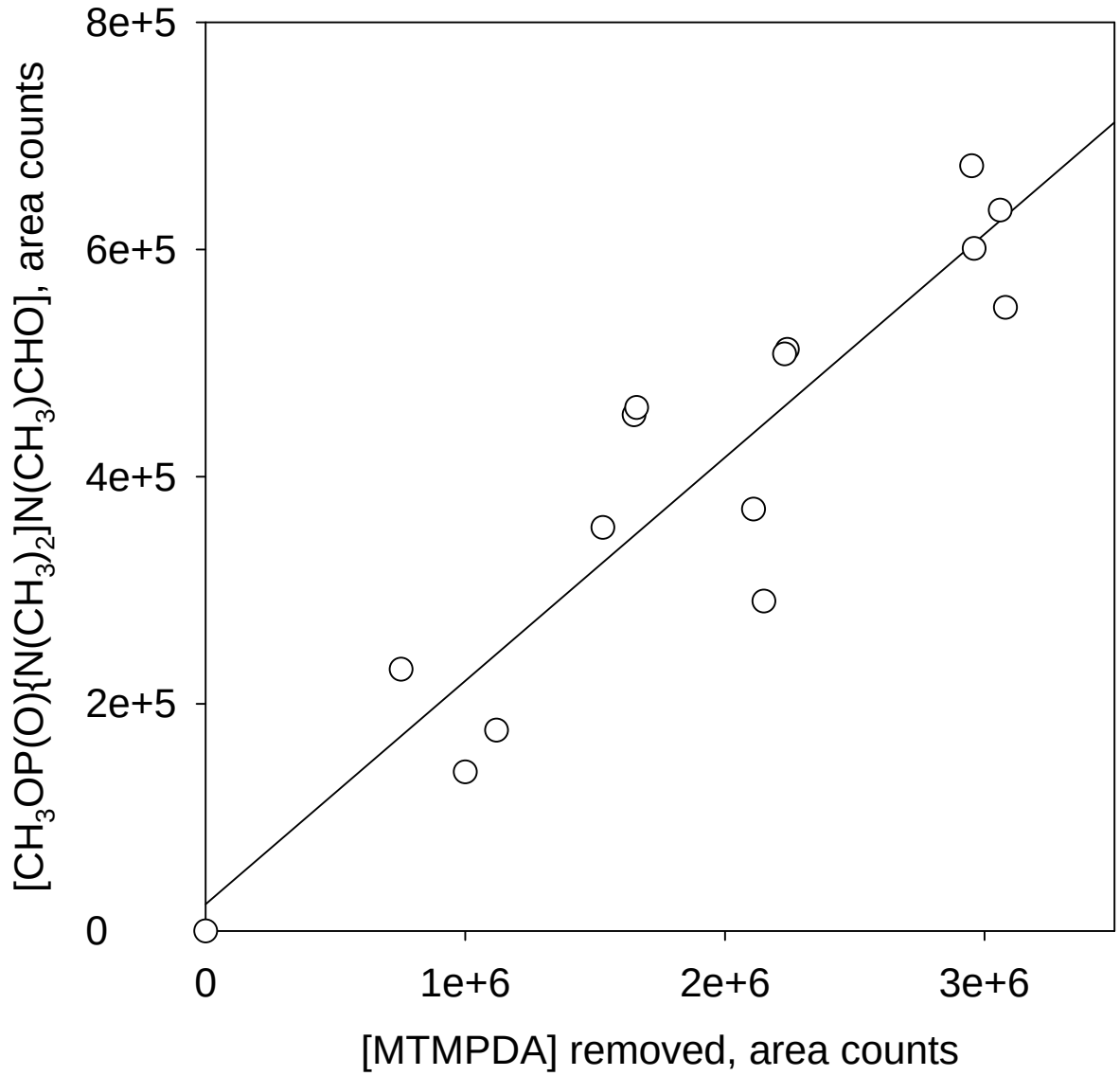

Figure S1. Plot of the GC-FID area counts of $CH_3OP(O)[N(CH_3)_2]N(CH_3)CHO$ formed against the GC-FID area counts of MTMPDA removed by reaction with NO_3 radicals and by dark decay. The plotted data have not been corrected for differences in GC-FID response (see text) or for the small contribution to the MTMPDA lost by dark decay.

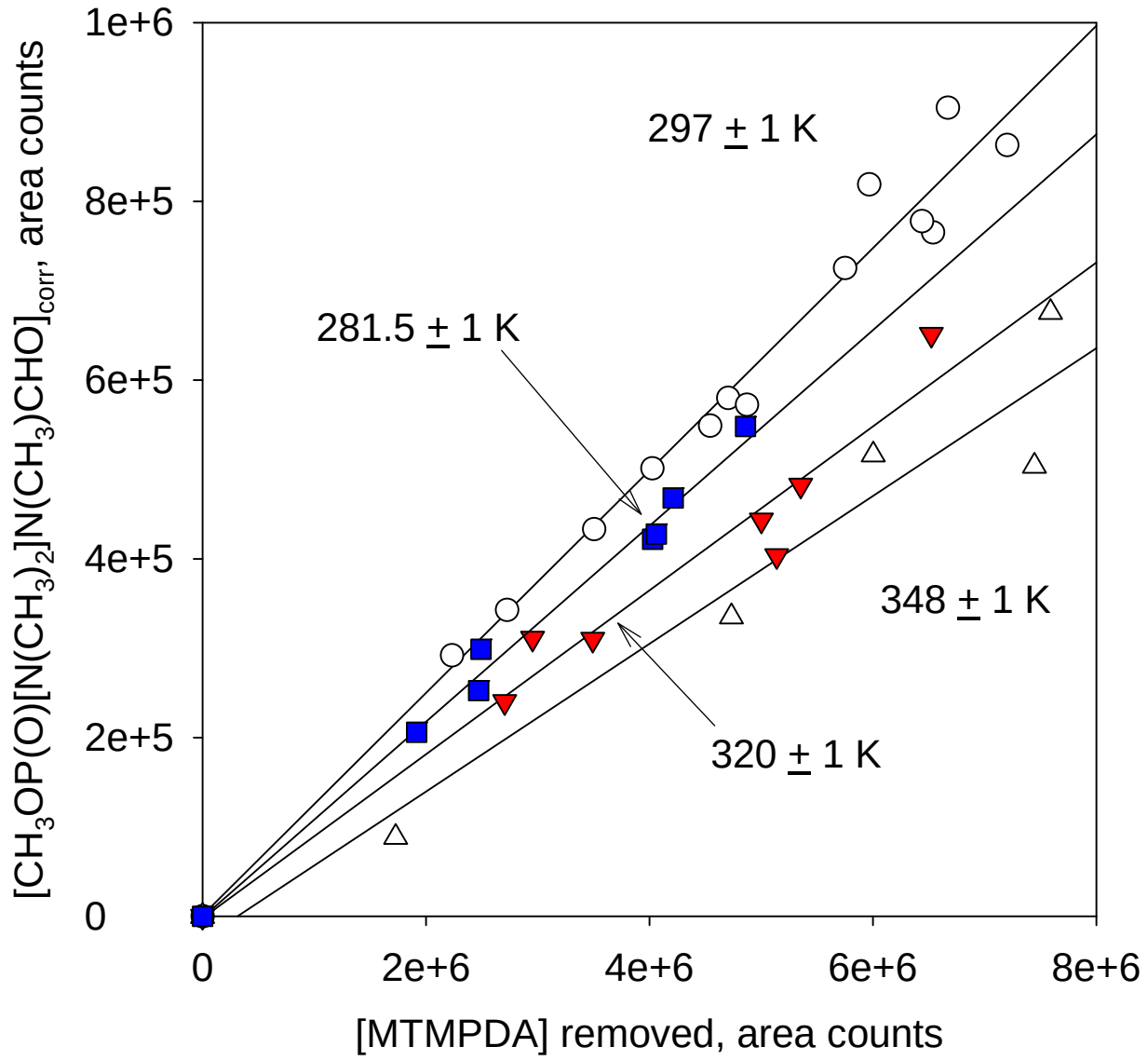

Figure S2. Plots of the GC-FID area counts of $CH_3OP(O)[N(CH_3)_2]N(CH_3)CHO$ formed, corrected for losses (reactive loss and dark decay) against the GC-FID area counts of MTMPDA removed by reaction with OH radicals and by dark decay. The plotted data have not been corrected for differences in GC-FID response (see text) or for the small contribution to the MTMPDA lost by dark decay. For details of the corrections for losses of $CH_3OP(O)[N(CH_3)_2]N(CH_3)CHO$, see the text.

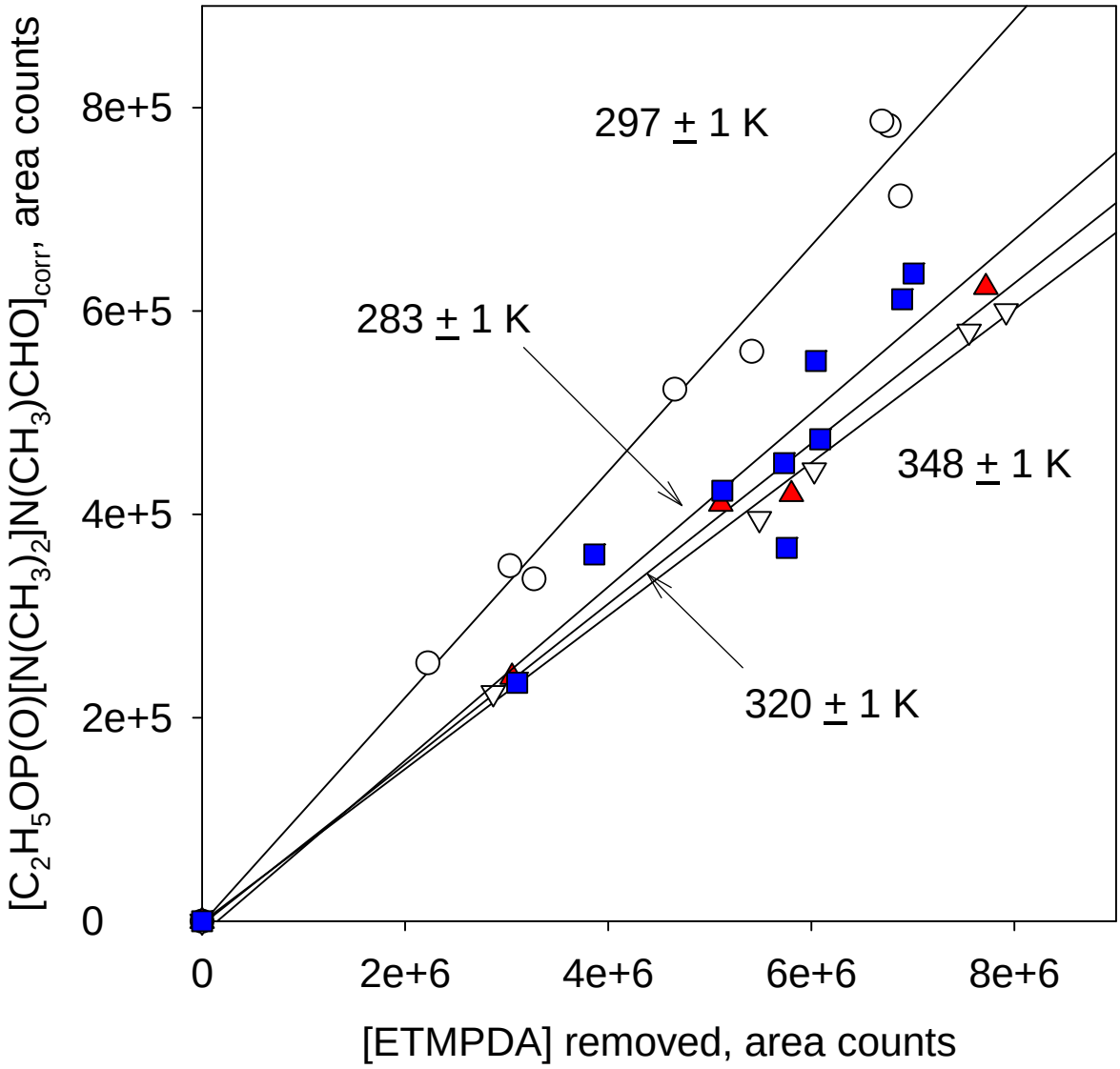

Figure S3. Plots of the GC-FID area counts of $C_2H_5OP(O)[N(CH_3)_2]N(CH_3)CHO$ formed, corrected for losses (reactive loss and dark decay) against the GC-FID area counts of ETMPDA removed by reaction with OH radicals and by dark decay. The plotted data have not been corrected for differences in GC-FID response (see text) or for the small contribution to the ETMPDA lost by dark decay. For details of the corrections for losses of $C_2H_5OP(O)[N(CH_3)_2]N(CH_3)CHO$, see the text.